

Ternary fission of $^{250,252}\text{Cf}$ isotopes with ^3H and ^6He as light charged particle

Sreejith Krishnan¹, K. P. Santhosh¹

¹(School of Pure and Applied Physics, Kannur University, Swami Anandatheertha Campus, Payyanur 670327, Kerala, India)

Abstract: The spontaneous cold ternary fission of $^{250,252}\text{Cf}$ isotope with ^3H and ^6He as light charged particle with fragments in equatorial and collinear configuration have been studied using the Unified ternary fission model (UTFM). In both equatorial and collinear configuration, the fragment combinations with the highest relative yield are found to be the same. In the ^3H accompanied ternary fission of ^{250}Cf and ^{252}Cf isotope, the highest relative yield is found for the ternary splitting $^{114}\text{Pd}+^3\text{H}+^{133}\text{Sb}$ and $^{116}\text{Pd}+^3\text{H}+^{133}\text{Sb}$ respectively. Here the fragment combinations possess the highest Q value and includes the presence of near doubly magic nucleus ^{133}Sb ($N=82, Z=51$). In the case of ^{250}Cf and ^{252}Cf isotope with ^6He as light charged particle, the highest relative yield is found for the fragmentation $^{110}\text{Ru}+^6\text{He}+^{134}\text{Te}$ and $^{114}\text{Pd}+^6\text{He}+^{132}\text{Sn}$ respectively, which is due to the presence of near doubly magic nucleus ^{134}Te ($N=82, Z=52$) and doubly magic nucleus ^{132}Sn ($N=82, Z=50$). Hence the presence of high Q value and doubly or near doubly magic nucleus plays a significant role in the ternary fission of $^{250,252}\text{Cf}$ isotopes with ^3H and ^6He as light charged particle.

Keywords: Spontaneous fission, cold ternary fission, relative yield, unified ternary fission model.

I. Introduction

The splitting of a radioactive nucleus into three fragments is commonly referred to as ternary fission and in most cases; one of the fragments is very light compared to the main fission fragments. Hence the process of ternary fission is also referred to as light charged particle (LCP) accompanied ternary fission. In 1947 Farewell *et al.*, [1] reported the experimental observation of ternary fission process in the case of uranium isotope. The process of ternary fission is found to occur for every once in 500 binary fission events with alpha particle as light charged particle and the observed alpha particle is found to emit in a direction perpendicular to the main fission fragments. Depending on the emission of light charged particle, mainly there are two different configurations in a ternary fission process namely, equatorial and collinear configuration. An equatorial configuration is one in which the light charged particle is emitted in a direction perpendicular to the main fission fragments. In the case of collinear configuration, the light charged particle is emitted along the direction of the main fission fragments. A number of theoretical and experimental works have been conducted in the field of ternary fission of various isotopes. We have developed a model named as Unified ternary fission model (UTFM) [2-7], in order to find the most favourable fragment combinations in the ternary fission process of various isotopes and our model is briefly described in the following section.

II. Unified ternary fission model (UTFM)

The light charged particle accompanied ternary fission is energetically possible only if Q value of the reaction is positive. ie.

$$Q = M - \sum_{i=1}^3 m_i > 0 \quad (1)$$

Here M is the mass excess of the parent and m_i is the mass excess of the fragments. The interacting potential barrier for a parent nucleus exhibiting cold ternary fission consists of Coulomb potential and nuclear proximity potential of Blocki *et al.*, [8, 9]. The interacting potential barrier is given by,

$$V = \sum_{i=1}^3 \sum_{j>i}^3 (V_{Cij} + V_{Pij}) \quad (2)$$

with $V_{Cij} = \frac{Z_i Z_j e^2}{r_{ij}}$, the Coulomb interaction between the fragments. Here Z_i and Z_j are the atomic numbers of

the fragments and r_{ij} is the distance between fragment centres. The nuclear proximity potential [8] between the fragments is,

$$V_{p_{ij}}(z) = 4\pi b \left[\frac{C_i C_j}{(C_i + C_j)} \right] \Phi \left(\frac{z}{b} \right) \quad (3)$$

Here Φ is the universal proximity potential and z is the distance between the near surfaces of the fragments. The distance between the near surfaces of the fragments for equatorial configuration is considered as $z_{12} = z_{23} = z_{13} = z$ and for collinear configuration the distance of separation are $z_{12} = z_{23} = z$ and $z_{13} = 2(C_2 + z)$. The Süßmann central radii C_i of the fragments related to sharp radii R_i is,

$$C_i = R_i - \left(\frac{b^2}{R_i} \right) \quad (4)$$

For R_i we use semi empirical formula in terms of mass number A_i as [8]

$$R_i = 1.28A_i^{1/3} - 0.76 + 0.8A_i^{-1/3} \quad (5)$$

The nuclear surface tension coefficient called Lysekil mass formula is given as,

$$\gamma = 0.9517[1 - 1.7826(N - Z)^2 / A^2] \text{ MeV/fm}^2 \quad (6)$$

where N , Z and A represents the neutron, proton and mass number of the parent, Φ , the universal proximity potential is given as,

$$\Phi(\varepsilon) = -4.41e^{-\varepsilon/0.7176}, \text{ for } \varepsilon > 1.9475 \quad (7)$$

$$\Phi(\varepsilon) = -1.7817 + 0.9270\varepsilon + 0.0169\varepsilon^2 - 0.05148\varepsilon^3, \text{ for } 0 \leq \varepsilon \leq 1.9475 \quad (8)$$

with $\varepsilon = z/b$, where the width (diffuseness) of the nuclear surface $b \approx 1$ fermi.

Using one-dimensional WKB approximation, the barrier penetrability P , probability for which the ternary fragments to cross the three body potential barrier is given as,

$$P = \exp \left\{ -\frac{2}{\hbar} \int_{z_1}^{z_2} \sqrt{2\mu(V - Q)} dz \right\} \quad (9)$$

The turning points $z_1=0$ represent touching configuration and z_2 is determined from the equation $V(z_2)=Q$, where Q is the decay energy. The potential V in eqn. 9, which is the sum of Coulomb and proximity potential given by eqn. 2, are computed by varying the distance between the near surfaces of the fragments. In eqn. 9 the mass parameter is replaced by reduced mass μ and is defined as,

$$\mu = m \left(\frac{\mu_{12} A_3}{\mu_{12} + A_3} \right) \text{ and } \mu_{12} = \frac{A_1 A_2}{A_1 + A_2} \quad (10)$$

where m is the nucleon mass and A_1 , A_2 and A_3 are the mass numbers of the three fragments.

The relative yield can be calculated as the ratio between the penetration probability of a given fragmentation over the sum of penetration probabilities of all possible fragmentation as follows,

$$Y(A_i, Z_i) = \frac{P(A_i, Z_i)}{\sum P(A_i, Z_i)} \quad (11)$$

III. Results and discussion

The cold ternary fission of $^{250,252}\text{Cf}$ isotope with ^3H and ^6He as light charged particle in both equatorial and collinear configuration of fragments have been studied using the concept of cold reaction valley, which was introduced in relation to the structure of minima in the so called driving potential. The driving potential is defined as the difference between the interaction potential V and the decay energy Q of the reaction. Here the interaction potential V is taken as the sum of Coulomb potential and nuclear proximity potential. The Q values are calculated using the recent mass tables of Wang *et al.*, [10] and for which the experimental values are not available; we have taken the values from the mass tables of Koura *et al.*, [11]. For a fixed light charged particle, the driving potential can be calculated for all possible fragment combinations as a function of mass and charge

asymmetries given as $\eta = \frac{A_1 - A_2}{A_1 + A_2}$ and $\eta_Z = \frac{Z_1 - Z_2}{Z_1 + Z_2}$ respectively. A pair of charges is singled out for every

fixed mass pair (A_1, A_2) in which the driving potential is minimized. The schematic diagram for the equatorial and collinear emission of three spherical fragments at the touching configuration is shown in figure 1.

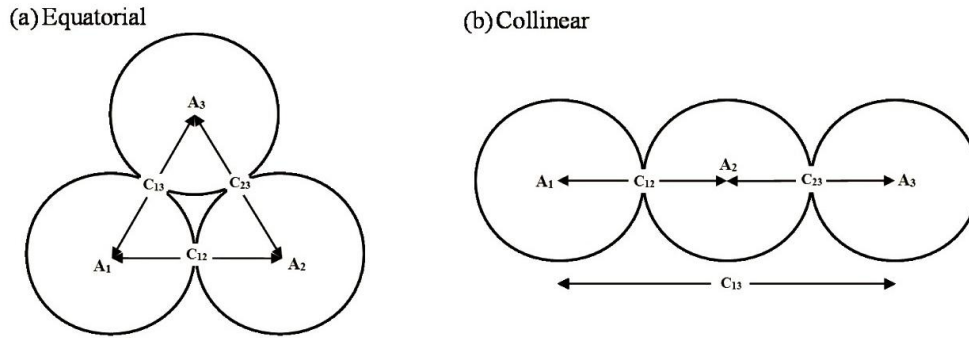


Fig.1. Schematic diagram for the touching configuration of the three spherical fragments formed in the process of ternary fission with fragments in (a) equatorial and (b) collinear configuration.

3.1 ^3H accompanied ternary fission of $^{250,252}\text{Cf}$ isotopes with fragments in equatorial configuration.

The spontaneous cold ternary fission of ^{250}Cf and ^{252}Cf isotopes has been studied with ^3H as light charged particle using the Unified ternary fission model (UTFM). In the ^3H accompanied ternary fission of ^{250}Cf isotope, the driving potential is calculated for all possible fragment combinations. Figure 2(a) represents the plot of driving potential versus fragment mass number A_1 found in the ternary fission of ^{250}Cf isotope with ^3H as light charged particle. Here the minimum is found for the fragment combination with fragment mass number $A_1 = ^8\text{Be}, ^{11}\text{B}, ^{12}\text{B}, ^{13}\text{B}, ^{14}\text{C}, ^{15}\text{C}, ^{16}\text{C}, ^{17}\text{N}, ^{18}\text{C}, ^{19}\text{N}, ^{20}\text{O}, ^{21}\text{O}, ^{22}\text{O}, ^{23}\text{F}, ^{24}\text{Ne}$ etc. The minimum found for the fragment combination $^{40}\text{S} + ^3\text{H} + ^{207}\text{Tl}$ is due to the presence of near doubly magic nucleus ^{207}Tl ($N=126, Z=81$). The minimum found around the fragment combination $^{82}\text{Ge} + ^3\text{H} + ^{165}\text{Tb}$ is due to the presence of neutron magic number $N=50$ of ^{82}Ge .

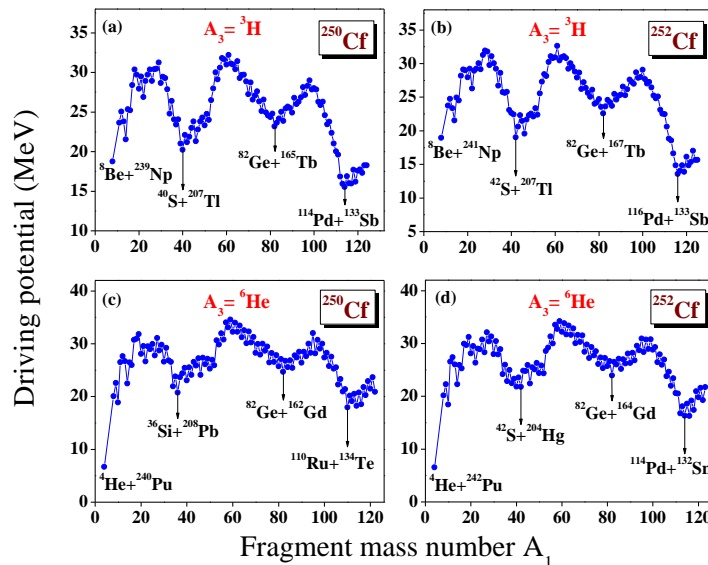


Fig.2. The driving potential is plotted as a function of fragment mass number A_1 in the case of ^3H and ^6He accompanied ternary fission of $^{250,252}\text{Cf}$ isotopes with fragments in equatorial configuration.

The deepest minimum found around the fragment combination $^{114}\text{Pd} + ^3\text{H} + ^{133}\text{Sb}$ is due to the presence of near doubly magic nucleus ^{133}Sb ($N=82, Z=51$), which may be the most suitable fragment combination in this ternary fission process. This can be verified through the calculation of barrier penetrability and the relative yield of fragment combinations obtained in the cold reaction valley. The barrier penetrability and hence the relative yield is calculated for each fragment combination found in the cold reaction valley plot. Figure 3(a) represents the relative yield plotted as a function of fragment mass numbers A_1 and A_2 . From the plot, it is clear that the highest relative yield is obtained for the fragment combination $^{114}\text{Pd} + ^3\text{H} + ^{133}\text{Sb}$, which includes the presence of near doubly magic nucleus ^{133}Sb . The second highest relative yield is obtained for the fragment combination $^{117}\text{Ag} + ^3\text{H} + ^{130}\text{Sn}$, which includes the presence of near doubly magic nucleus ^{130}Sn ($N=80, Z=50$). The next highest relative yield is obtained for the fragment combination $^{119}\text{Ag} + ^3\text{H} + ^{128}\text{Sn}$ which includes the presence of proton shell closure $Z=50$ of ^{128}Sn .

In the ^3H accompanied ternary fission of ^{252}Cf isotope, the driving potential is calculated and plotted as a function of fragment mass number A_1 as shown in figure 2(b). Here the deepest minimum is found for the fragment combination $^{116}\text{Pd}+^3\text{H}+^{133}\text{Sb}$, which includes the presence of near doubly magic nucleus ^{133}Sb ($N=82$, $Z=51$). The minima found around the fragment combinations $^{42}\text{S}+^3\text{H}+^{207}\text{Tl}$ and $^{82}\text{Ge}+^3\text{H}+^{167}\text{Tb}$ are due to the presence of near doubly magic nucleus ^{207}Tl ($N=126$, $Z=81$) and neutron shell closure $N=50$ of ^{82}Ge respectively. The relative yield is calculated for all possible fragmentations and plotted as a function of fragment mass numbers A_1 and A_2 as shown in figure 3(b). From the plot, it is clear that the highest relative yield is found for the fragment combination $^{116}\text{Pd}+^3\text{H}+^{133}\text{Sb}$, which is the same fragment combination with least driving potential in the cold reaction valley plot. Also the fragment combination possess the presence of near doubly magic nucleus ^{133}Sb ($N=82$, $Z=51$). The next highest relative yield found for the fragment combination $^{119}\text{Ag}+^3\text{H}+^{130}\text{Sn}$ is due to the presence of near doubly magic nucleus ^{130}Sn ($N=80$, $Z=50$). The presence of doubly magic nucleus ^{132}Sn and high Q value makes the fragment splitting $^{117}\text{Ag}+^3\text{H}+^{132}\text{Sn}$ a more probable one in this ternary fission process.

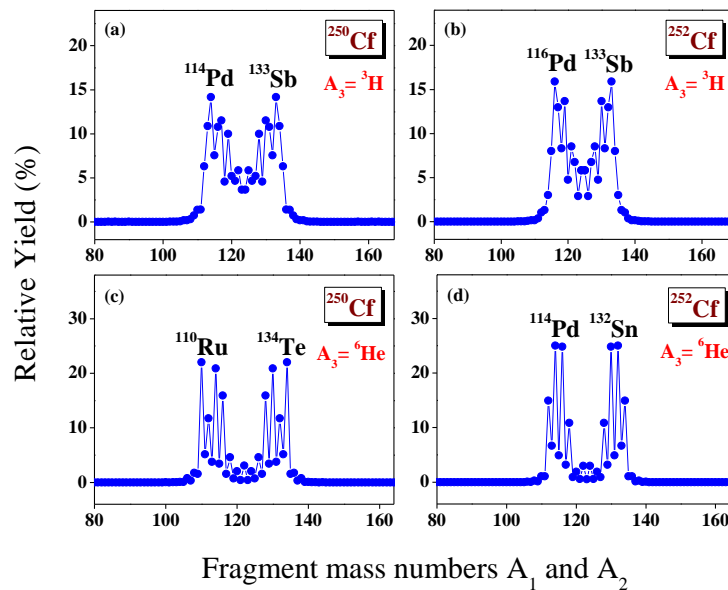


Fig.3. The relative yield is plotted as a function of fragment mass numbers A_1 and A_2 in the case of ^3H and ^6He accompanied ternary fission of $^{250,252}\text{Cf}$ isotopes with fragments in equatorial configuration.

3.2 ^6He accompanied ternary fission of $^{250,252}\text{Cf}$ isotopes with fragments in equatorial configuration

For the ^{250}Cf isotope with ^6He as light charged particle, the driving potential is calculated for all possible fragmentations and plotted as a function of fragment mass number A_1 as shown in figure 2(c). Here the deepest minimum is found for the fragment combination $^4\text{He}+^6\text{He}+^{240}\text{Pu}$, which possess doubly magic nucleus ^4He and a low Q value. The next minimum is found around the fragment combination $^{110}\text{Ru}+^6\text{He}+^{134}\text{Te}$, which includes the presence of near doubly magic nucleus ^{134}Te ($N=82$, $Z=52$). The same fragment combination possesses the highest Q value and hence may be the most suitable fragment splitting in this ternary fission process. The relative yield is calculated for all possible fragmentations and plotted as a function of fragment mass numbers A_1 and A_2 as shown in figure 3(c). In this case, the highest relative yield is found for the fragment combination $^{110}\text{Ru}+^6\text{He}+^{134}\text{Te}$, which includes the presence of near doubly magic nucleus ^{134}Te ($N=82$, $Z=52$). The next higher relative yields are found for the fragment combinations $^{114}\text{Pd}+^6\text{He}+^{130}\text{Sn}$ and $^{116}\text{Pd}+^6\text{He}+^{128}\text{Sn}$, which include the presence of near doubly magic nucleus ^{130}Sn ($N=80$, $Z=50$) and proton shell closure $Z=50$ of ^{128}Sn respectively.

In the ^6He accompanied ternary fission of ^{252}Cf isotope, the driving potential is calculated for all possible fragmentations and plotted as a function of fragment mass number A_1 as shown in figure 2(d). Here the deepest minimum is found for the fragment combination $^4\text{He}+^6\text{He}+^{242}\text{Pu}$. The next minimum found for the fragment combination around $^{114}\text{Pd}+^6\text{He}+^{132}\text{Sn}$ is due to the presence of doubly magic nucleus ^{132}Sn ($N=82$, $Z=50$). The relative yield is calculated and plotted as a function of fragment mass numbers A_1 and A_2 as shown in figure 3(d). From the plot, the highest relative yield is found for the fragment combination $^{114}\text{Pd}+^6\text{He}+^{132}\text{Sn}$, which is the same fragment combination with high Q value and also possess the presence of doubly magic

nucleus ^{132}Sn (N=82, Z=50). The next higher relative yields are found for the ternary splitting $^{116}\text{Pd}+^6\text{He}+^{130}\text{Sn}$ and $^{112}\text{Ru}+^6\text{He}+^{134}\text{Te}$, of which ^{130}Sn (N=80, Z=50) and ^{134}Te (N=82, Z=52) are near doubly magic nuclei.

3.3 ^3H accompanied ternary fission of $^{250,252}\text{Cf}$ isotopes with fragments in collinear configuration

In the ^3H accompanied ternary fission of ^{250}Cf and ^{252}Cf isotopes with fragments in collinear configuration the driving potential is plotted as a function of fragment mass number A_1 as shown in figure 4(a) and 4(b) respectively. The fragment combinations with least driving potential are also labeled. The relative yield in the case of ^{250}Cf and ^{252}Cf are calculated for all possible fragmentations found in the cold reaction valley and plotted as shown in figure 5(a) and 5(b) respectively. In the case of ^{250}Cf isotope, the highest relative yield is obtained for the ternary splitting $^{114}\text{Pd}+^3\text{H}+^{133}\text{Sb}$, which possess near doubly magic nucleus (N=82, Z=51). The next higher relative yields found in the ^3H accompanied ternary fission of ^{250}Cf are for the fragment combinations $^{117}\text{Ag}+^3\text{H}+^{130}\text{Sn}$ and $^{116}\text{Pd}+^3\text{H}+^{131}\text{Sb}$. In the case of ^{252}Cf isotope, the highest relative yield is found for the fragment combination $^{116}\text{Pd}+^3\text{H}+^{133}\text{Sb}$, which includes the presence of doubly magic nucleus ^{133}Sb . The fragment combinations $^{119}\text{Ag}+^3\text{H}+^{130}\text{Sn}$ and $^{117}\text{Ag}+^3\text{H}+^{132}\text{Sn}$ also possess a higher relative yields in the ternary fission of ^{252}Cf isotope with ^3H as light charged particle formed in collinear configuration.

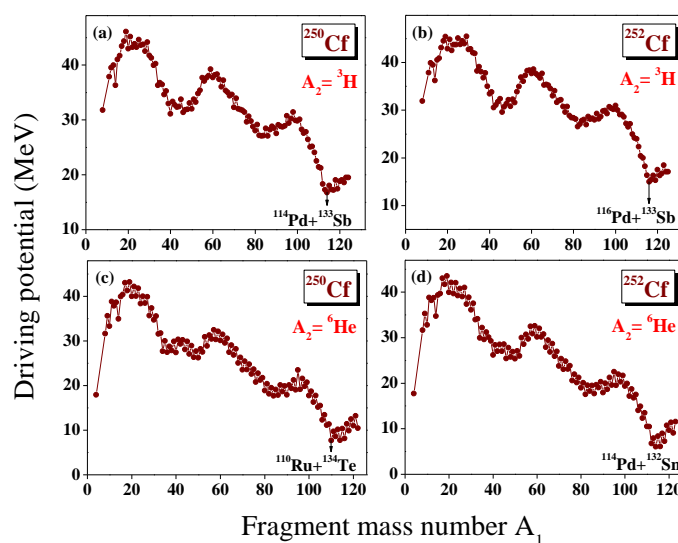


Fig.4. The driving potential is plotted as a function of fragment mass number A_1 in the case of ^3H and ^6He accompanied ternary fission of $^{250,252}\text{Cf}$ isotopes with fragments in collinear configuration.

3.4 ^6He accompanied ternary fission of $^{250,252}\text{Cf}$ isotopes with fragments in collinear configuration

In the ^6He accompanied ternary fission of ^{250}Cf and ^{252}Cf isotopes with fragments in collinear configuration the driving potential is plotted as a function of fragment mass number A_1 as shown in figure 4(c) and 4(d) respectively. The relative yield is calculated for all fragment combinations found in the cold reaction valley plot. Figure 5(c) and 5(d) represents the relative yield versus fragment mass numbers A_1 and A_3 in the case of ^{250}Cf and ^{252}Cf isotopes respectively. For ^{250}Cf isotope, the highest relative yield is found for the splitting $^{110}\text{Ru}+^6\text{He}+^{134}\text{Te}$, which includes near doubly magic nucleus ^{134}Te . The next higher relative yields are found for $^{114}\text{Pd}+^6\text{He}+^{130}\text{Sn}$, $^{116}\text{Pd}+^6\text{He}+^{128}\text{Sn}$ and $^{112}\text{Pd}+^6\text{He}+^{132}\text{Sn}$. For the ^{252}Cf isotope, the fragment combination $^{114}\text{Pd}+^6\text{He}+^{132}\text{Sn}$ has the highest relative yield, which includes doubly magic nucleus ^{132}Sn . The next higher relative yields are found for the splitting $^{116}\text{Pd}+^6\text{He}+^{130}\text{Sn}$, $^{112}\text{Ru}+^6\text{He}+^{134}\text{Te}$, $^{118}\text{Pd}+^6\text{He}+^{128}\text{Sn}$.

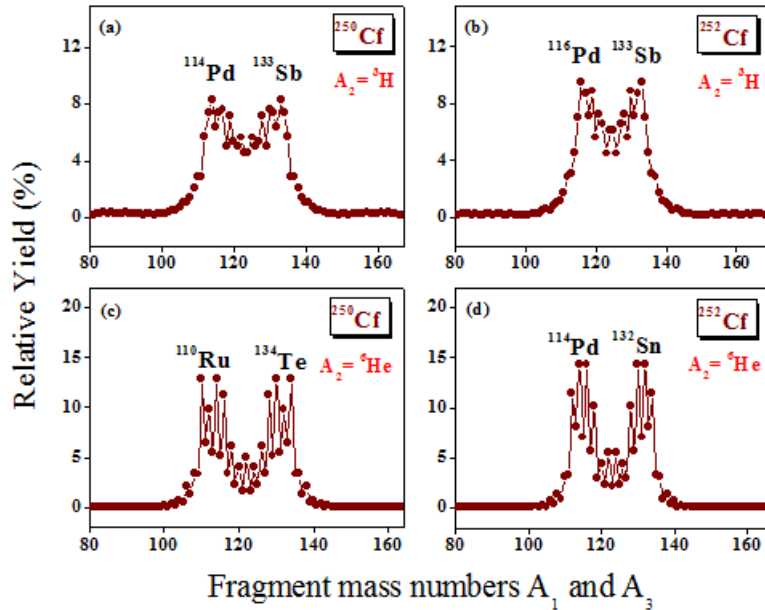


Fig.5. The relative yield is plotted as a function of fragment mass numbers A_1 and A_3 in the case of ^3H and ^6He accompanied ternary fission of $^{250,252}\text{Cf}$ isotopes with fragments in collinear configuration.

IV. Conclusion

Using Unified ternary fission model (UTFM), the spontaneous cold ternary fission of $^{250,252}\text{Cf}$ isotopes with ^3H and ^6He as light charged particle with fragments in equatorial and collinear configuration has been studied. The fragment combinations with the highest relative yield are found to be the same in both equatorial and collinear configuration. In the ^3H accompanied ternary fission of ^{250}Cf and ^{252}Cf isotope, the most probable fragmentation is found for $^{114}\text{Pd}+^3\text{H}+^{133}\text{Sb}$ and $^{116}\text{Pd}+^3\text{H}+^{133}\text{Sb}$ respectively, in which ^{133}Sb ($N=82$, $Z=51$) is a near doubly magic nucleus. In the ternary fission of ^{250}Cf and ^{252}Cf isotope with ^6He as light charged particle, the most probable fragmentation is found for $^{110}\text{Ru}+^6\text{He}+^{134}\text{Te}$ and $^{114}\text{Pd}+^6\text{He}+^{132}\text{Sn}$ respectively, which is due to the presence of near doubly magic nucleus ^{134}Te ($N=82$, $Z=52$) and doubly magic nucleus ^{132}Sn ($N=82$, $Z=50$). Hence we can conclude that in the ternary fission of $^{250,252}\text{Cf}$ isotopes with ^3H and ^6He as light charged particle, the presence of doubly or near doubly magic nucleus and high Q value plays an important role.

Acknowledgements

The author KPS would like to thank the University Grants Commission, Govt. of India for the financial support under Major Research Project. No.42-760/2013 (SR) dated 22-03-2013.

References

- [1]. G. Farewell, E. Segre and C. Wiegand, Long range alpha-particles emitted in connection with fission. Preliminary Report, *Physical Review*, 71(6), 1947, 327-330.
- [2]. K. P. Santhosh, Sreejith Krishnan and B. Priyanka, Light charged particle accompanied ternary fission of ^{242}Cm using the Coulomb and proximity potential, *The European Physical Journal A*, 50(4), 2014, 66.
- [3]. K. P. Santhosh, Sreejith Krishnan and B. Priyanka, The emission probabilities of long range alpha particles from even-even $^{244-252}\text{Cm}$ isotopes, *Journal of Physics G: Nuclear and Particle Physics*, 41(10), 2014, 105108.
- [4]. K. P. Santhosh, Sreejith Krishnan and B. Priyanka, ^{34}Si accompanied ternary fission of ^{242}Cm in equatorial and collinear configuration, *International Journal of Modern Physics E*, 23(11), 2014, 1450071.
- [5]. K. P. Santhosh, Sreejith Krishnan and B. Priyanka, Isotopic yield in alpha accompanied ternary fission of ^{252}Cf , *International Journal of Modern Physics E*, 24(01), 2015, 1550001.
- [6]. K. P. Santhosh, Sreejith Krishnan and B. Priyanka, α -accompanied cold ternary fission of $^{238-244}\text{Pu}$ isotopes in equatorial and collinear configuration, *Physical Review C*, 91(4), 2015, 044603.
- [7]. K. P. Santhosh and Sreejith Krishnan, Deformation effects in the alpha accompanied cold ternary fission of even-even $^{244-260}\text{Cf}$ isotopes, *The European Physical Journal A*, 52(4), 2016, 108.
- [8]. J. Blocki, J. Randrup, W. J. Swiatecki, C. F. Tsang, Proximity forces, *Annals of Physics*, 105(2), 1977, 427-462.
- [9]. J. Blocki, W. J. Swiatecki, A generalization of the proximity force theorem, *Annals of Physics*, 132(1), 1983, 53-65.
- [10]. M. Wang, G. Audi, A. H. Wapstra, F. G. Kondev, M. MacCormick, X. Xu and B. Pfeiffer, The AME 2012 atomic mass evaluation, *Chinese Physics C*, 36(12), 2012, 1603-2014.
- [11]. H. Koura, T. Tachibana, M. Uno and M. Yamada, Nuclidic mass formula on a spherical basis with an improved even-odd term, *Progress of Theoretical Physics*, 113(2), 2005, 305-325.